ICAS-88-2.2.2

DESIGN PHILOSOPHY OF LONG RANGE LFC TRANSPORTS WITH ADVANCED SUPERCRITICAL LFC AIRFOILS

Werner Pfenninger* and Chandra S. Vemuru**
Analytical Services & Materials Inc.,
Hampton, Virginia, U.S.A.

Abstract

Large span wings and 70% laminar flow over wing, struts, empennage and nacelles (fuselage turbulent) enable cruise lift to drag ratios (L/D) of 39 and 35 for cruise Mach number (M_{cruise}) = 0.83 and 0.97 Laminar Flow Control (LFC) airplanes. The corresponding ranges are 21,564 Km and 19,750 Km, assuming 180000 Kg take-off gross weight (W_o), 50000 Kg payload and $0.38 \times W_o$ gross weight empty for both airplanes and 0.48 Kg/Kg thrust specific fuel consumption at free-stream Mach number (M_∞) = 0.83 and a 3% higher $\eta_{overall}$ for the M_∞= 0.97 airplane.

Supercritical (SC) LFC airfoils with undercut front and rear lower surfaces and upper surface C_p- distribution with an extensive low supersonic flat rooftop, a far upstream supersonic pressure minimum and a steep subsonic rear pressure rise with suction or a slotted cruise flap raise $M_{\infty_{Design}}$ and reduce wing sweep to alleviate sweep-induced crossflow- and attachment line boundary layer instability.

Taper on swept-back wings adds a streamwise flow deceleration (assuming equal $M_\perp$ (normal to the isobars) as on a constant chord wing), aggravating laminarization and requiring additional suction on the upper surface rooftop to control Tollmien-Schlichting (TS)-disturbances. This effect is opposite for tapered swept-forward LFC wings. Their structural sweep is smaller than the isobar sweep at the start of the rear pressure rise (i.e.the shock sweep) to somewhat increase span and reduce induced drag. Sweeping the bending fibers of swept-forward composite wings ahead of the elastic axis, sweeping back the outboard wings and actively deflecting the cruise flap and fuel nacelle control surface eliminates wing divergence.

Wing-mounted superfans and with a fuselage boundary layer propulsion engine reduce fuel consumption and engine tone noise in the frequency range of amplified boundary layer disturbances.

Notation

A	Boundary layer disturbance amplitude
A_O	Initial disturbance amplitude
a	Sound velocity
C_{D_∞}	Equivalent profile drag coefficient of low drag suction wing
C_L	Lift coefficient
$C_{m_{c/4}}$	Airfoil pitching moment (with respect to c/4)
$C_p = \frac{2p}{\rho U_\infty^2}$	Surface static pressure coefficient
$\Delta C_p = \frac{2\Delta p}{\rho U_\infty^2}$	Nondimensional surface static pressure jump across off-design flow discontinuities and shocks
$C_Q = \frac{\rho_{wall}\, v_o}{\rho_{amb.}\, U_{flight}}$	Nondimensional suction mass-flow coefficient
c	Airfoil chord
h	Height of supersonic bubble
l	Length of supersonic bubble
M_∞	Free-stream Mach number
$N = ln(A/A_O)$	logarithmic growth factor of amplified boundary layer disturbances
Re_c	Wing chord Reynolds number
$Re_n = \frac{w_{max}\,\delta_{0.1}}{\nu}$	Boundary layer cross flow Reynolds number (based on w_{max} and boundary layer thickness $\delta_{0.1}$ where $w = 0.1 \times w_{max}$)
t/c	Airfoil thickness ratio
U_∞	Free-stream velocity (normal to leading edge)
U_{flight}	Flight speed
v_o	Equivalent area suction velocity
w	Boundary layer crossflow velocity
$\chi = (\frac{W_{max}\,\delta_{0.1}}{\nu})$	Boundary layer crossflow stability limit Reynolds number
x	Chordwise distance
y	Vertical coordinate
α	Effective wing angle of attack
$\beta_{0.115}$	Deflection of 0.115 chord trailing edge cruise flap
φ	Wing sweep angle
μ	Absolute viscosity
ν	Kinematic viscosity

* Senior Research Scientist, AS&M Inc., Associate Fellow AIAA.
** Research Engineer, AS&M Inc., Member AIAA.

A. Introduction, formulation of goal, overall design approaches

With the interest in long range air transportation the question arises concerning the design philosophy of long range LFC transports, which can reach any point on earth at high subsonic speeds with relatively large payloads without refuelling. Figure 1 shows as an example a 180,000 kg take-off gross weight LFC transport airplane with 50,000 kg payload (250 passengers plus cargo) cruising at M_{cruise}= 0.83. Cruise lift to drag ratios of 39.4 appear feasible with 70% laminar flow on the wing-, tail-, nacelle- and strut surfaces by means of suitable geometry and boundary layer suction in the upstream parts of these surfaces, while accepting a turbulent fuselage. At the same time the induced drag to lift ratio $D_i/L = W/\pi q b^2$ is minimized by raising the wing span b and aspect ratio b^2/S. Advanced overall and detailed design concepts were used to minimize the wing structural weight [Ref.1].

The design philosophy leading to this airplane layout will now be discussed in more detail. The airplane range $R = \eta_{ov} \times L/D \times H \times ln(W_A/W_E)$ is proportional to the airplane lift to drag ratio L/D, the overall efficiency η_{ov} of the airplane propulsion system and the log of the airplane weight ratio W_A/W_E between start and end of cruise (H = specific heat content of fuel). Assuming for simplicity constant airplane zero lift drag $C_{D_o}= C_{D_\infty}+ C_{D_{parasite}}$ for different Re_c's and C_L's, the maximum L/D and corresponding optimum cruise lift coefficient $C_{L_{opt}}$ are: $(L/D)_{max} = \sqrt{\frac{\pi \times b^2/S}{4\, C_{D_o}}}$, $C_{L_{opt}} = \sqrt{\frac{\pi \times b^2}{S} \times C_{D_o}}$.

The variation of $\left(\frac{L}{D}\right)_{max}$ and $C_{L_{opt}}$ versus the laminar airplane wetted area ratio $A_{laminar}/A_{total}$ is shown in the Figures 2 and 3 [Ref. 2], assuming a linear decrease of C_{D_o} from 0.012 for the all turbulent airplane to 0.0020 for the fully laminar airplane with a relative fuselage size of a B52. $\left(\frac{L}{D}\right)_{max}$ grows progressively rapidly as $A_{laminar}/A_{total}$ increases, reaching phenomenally high values with fully laminar flow over the airplane exposed surfaces, especially with higher wing aspect ratios. $C_{L_{opt}}$ decreases with increasing $A_{laminar}/A_{total}$ ratios, raising accordingly the airplane design speed. This enables less wing sweep and thereby reduces sweep-induced boundary layer crossflow instability. Thus, to maximize L/D, C_{D_o} should be minimized by extensive airplane laminarization; furthermore, to obtain the full benefit from the lower laminar airplane friction drag, the airplane induced drag to lift ratio $D_i/L = W/\pi q b^2$ should be reduced simultaneously by lowering the span loading W/b^2, i.e. raising the wing span and with it the wing aspect ratio b^2/S, compatible with a low wing structural weight.

Besides pure performance considerations the design of large LFC airplanes is critically influenced by suction laminarization problems [Ref. 1]. Boundary layer stability problems are easier to handle at lower length Reynolds numbers. Also, the permissible surface roughness and tolerances for laminar flow are inversely proportional to the airplane unit length Reynolds number U_∞/ν. Therefore, larger LFC airplanes should preferably be designed such that performance optimization is compatible with the desire to alleviate the laminarization problems involved by reducing Re_c and U_∞/ν. Since $Re_c = \frac{U_\infty c}{\nu} = \frac{2W^{0.5}}{a\mu C_L M} \times \sqrt{\frac{W/S}{b^2/S}}$ and $\frac{U_\infty}{\nu} = \frac{2(W/S)}{a\mu C_L M}$ it follows that Re_c decreases by lowering the wing loading W/S, raising the wing aspect ratio b^2/S as well as C_L. Thus, the reduction of the induced drag to lift ratio $D_i/L = W/\pi q b^2$ by lowering the span loading W/b^2 for superior performance is well compatible with the desire to reduce $Re_c \approx \sqrt{W/b^2}$.

Design Approaches Towards Larger Span Wings With Reasonably Low Structural Weights [Refs. 1,2]

The desire to increase the wing span, while keeping the wing structural weight within bounds, profoundly influences the design of high performance LFC airplanes. Advanced overall and detail design approaches are needed for this purpose, borrowing if necessary design approaches of the past, which become attractive again in the light of new aerodynamic refinements. For example, the wing span can be substantially increased without sacrificing wing structural weight by bracing the wing externally by laminarized wide chord struts of low parasite drag (fig. 1), which take out the wing bending and torsional moments and deformations. Essentially, a rigid strut-braced inboard wing is thus added to a cantilever outer wing. Wing loads decrease further by placing an external laminarized fuel nacelle in the outer part of the wing and bracing it against the wing by laminarized struts. Wing gust-, maneuver- and dynamic loads and aeroelastic deformations and as a result wing structural weight decrease further by actively deflecting a small chord trailing edge cruise flap.

Such a cruise flap allows a variation of C_L at constant α_{wing}. When no suction is being considered in the rear pressure rise area of the upper surface a slotted cruise flap could enable a steeper pressure rise in this area than a plain cruise flap, resulting in a more extensive supersonic flat rooftop pressure distribution with laminar flow to raise accordingly $M_{\infty_{Design}}$ and lower

C_{D_∞}. Slotted SC wings were first proposed by Whitcomb [Ref. 3].

Aeroelastic wing torsional deformations can be alleviated by an active horizontal control surface located on a boom at the downstream end of the external fuel nacelle, which equalizes the wing angles of attack at the location of these nacelles and the wing root, using for example inertial platforms as sensors. Aeroelastic wing angle of attack changes induced by cruise flap deflection and swept wing bending and torsional deformation can be largely compensated by the active control surfaces of the fuel nacelles. Such an active control of the wing angle of attack along the span is particularly important for supercritical (SC) LFC wings, for which the flow in the embedded supersonic zone of the upper surface is especially sensitive to angle of attack changes.

In view of the high strength and stiffness of advanced composites, LFC airplanes in advanced composite structure are emphasized. Advanced SC airfoils with particularly high design Mach numbers minimize wing sweep for high subsonic speed airplanes to raise accordingly the wing span and reduce induced drag.

Drag Reduction of Wings and Bodies by Laminarization

The variation of the equivalent wing profile drag C_{D_∞} with transition location $(x/c)_T$ and Re_c is shown in figs. 4-5 for a 23^0 swept supercritical LFC wing. At $Re_c = 3\times10^7$ C_{D_∞} decreases from 0.0067 with fully turbulent flow to 0.0024 with 70% laminar flow and 0.0010 with 100% laminar flow (including $C_{D_{suction}}$). As compared to an unswept subcritical LFC wing, C_{D_∞} of the 23^0 swept SC LFC wing is somewhat larger especially at higher Re_c's (fig. 5). This is primarily a result of higher suction rates in the front and rear part of the wing for control of sweep-induced boundary layer crossflow instability.

Since the turbulent fuselage drag represents a large percentage drag contribution to an otherwise laminar LFC airplane the question arises concerning the possible suction laminarization of the fuselage at high length Reynolds numbers Re_L. Figure 6 shows Ames 12 ft. tunnel drag results of the Northrop Reichardt LFC body of revolution (8:1 fineness ratio, 12 ft. long) with $C_{D_{min}} = .00026$ (based on body wetted area, including $C_{D_{suction}}$) [Refs. 4,5]. This body drag reduction is percentage-wise larger than for all laminar flow wings and therefore rather tempting. The question then arises concerning the possible laminar flow Re_L-values of an LFC fuselage in flight at high subsonic speeds. In view of the practically non- existent atmospheric microscale turbulence, $Re_{L_{laminar}}$ of the Reichardt LFC body of revolution may be safely doubled to 120×10^6 for incompressible flow. The stabilizing influence of compressibility on the growth of amplified TS-waves may again double this value to 200×10^6 to 240×10^6 in flight at high subsonic cruising speeds.

For the present study a fully turbulent fuselage was assumed, applying a 7% and 10% equivalent fuselage drag reduction by riblets and fuselage boundary layer air propulsion in the rear part of the fuselage, respectively.

B. Laminarization Problems of Swept LFC Wings

Full chord laminar flow and low profile drags ($C_{D_\infty} = 0.0010$, including $C_{D_{suction}}$) have been obtained on a 30^0 swept LFC airfoil [Ref. 6]. Boundary layer crossflow instability and spanwise turbulent contamination along the front attachment line critically affect the design of more strongly swept LFC wings at higher Re_c's [Refs. 5-7]. The question, therefore, arises as to the alleviation of these sweep-induced boundary layer stability problems. In addition, 3-dimensional leading edge roughness (flyspecks, atmospheric ice crystals) is inherently more sensitive on swept laminar flow wings than without sweep: Besides higher local flow velocities in the leading edge region of the swept wing, the streamwise disturbance vorticity induced by 3-dimensional roughness superimposes adversely with the sweep- induced streamwise boundary layer disturbance vortices to precipitate transition. Indeed, leading edge flyspecks often caused extensive loss of laminar flow on the X-21 LFC wing with 33^0 swept leading edge at $M_\infty = .75$ and 12000 meters altitude [Ref. 8], while full chord laminar flow on the F94 LFC wing glove with 10^0 swept leading edge has been consistently observed at $M_\infty = .65$ and altitudes above 6000 meters to 7000 meters[Ref. 9]. Similarly, atmospheric ice crystal contamination had not been noticed on the F94 LFC glove, while often causing extensive loss of laminar flow on the X-21 wing [Ref. 8].

To alleviate these sweep- induced boundary layer stability problems wing sweep should be reduced by maximizing $M_{\infty_{Design}}$ of the airfoil, while maintaining a satisfactory off-design behavior and easing suction laminarization. This is possible for SC LFC airfoils with upper surface C_p-distributions with an extensive low supersonic flat rooftop, preceded by a far upstream supersonic pressure minimum and followed by a steep subsonic rear pressure rise to the trailing edge with low drag suction [Ref. 10]. $M_{\infty_{Design}}$ increases further by undercutting the front and rear lower airfoil surface, resulting in a relatively sharp leading edge [Ref. 10-

11]. To simplify the wing design and minimize the wing weight penalty due to LFC, suction should be limited as far as possible in the area of the main wing structure [Ref. 10].

Next, the suction requirements were studied for full chord suction laminarization at the design point of the SC airfoil X66 for $Re_c = 3.0 \times 10^7$ and 23^0 and 37^0 wing sweep, corresponding to $M_{flight} = 0.83$ and 0.98, respectively. This airfoil is a conservative derivative of airfoil X63T18S [Ref. 10]; its 2-dimensional design C_p-distribution and supersonic bubble are shown in the Korn Garabedian (KG)- plot of fig. 7 ($M_{\infty_{Design}} = 0.781$, $C_{L_{Design}} = 0.624$). The figs. 8,9 show as an example the C_p- and suction distribution and the corresponding growth of amplified boundary layer crossflow- and TS- disturbance vortices for the upper surface at $M_\infty = 0.98$ and $\varphi = 37^0$ sweep, using COSAL [Ref. 12].

No suction is needed for boundary layer crossflow control in the leading edge area for $\varphi = 23^0$ and $Re_c = 3.0 \times 10^7$. Increasing φ to 37^0 requires suction through a few closely spaced spanwise slots in a narrow strip of the front acceleration zone of the upper surface, where the crossflow is about neutrally stable and the corresponding flow Mach number varies from low to moderately high subsonic values.

Since the crossflow in the flow deceleration area downstream of the upper surface pressure minimum cancels the crossflow in the preceding acceleration zone, crossflow disturbance vortices and their interaction with amplified TS- waves are practically eliminated in the flat rooftop area. Weak suction ($C_q = -1.2 \times 10^{-4}$) from x/c = 0.05 to 0.30 is then adequate at the design point of X66 airfoil for boundary layer stabilization against TS-disturbances in the rooftop area of the upper surface at $Re_c = 3.0 \times 10^7$ (fig. 9). The strongly stabilizing influence of compressibility [Ref. 12] enables surprisingly large suction interruptions in the wing structural area, at least at the airfoil design condition. At off-design, small changes in M_∞ and α_{wing} add relatively severe flow decelerations for laminar flow in the rooftop area of the upper surface, as shown for example in fig. 10. Additional narrow suction strips may then be needed in the main wing box area for further TS- boundary layer stabilization.

The steep flow deceleration and relatively thick boundary layer in the rear pressure rise areas of the upper and lower surface generate a severe boundary layer crossflow, requiring strong suction in this area for boundary layer crossflow stabilization with full chord laminar flow (TS- instability is not critical). Less overall suction is needed for this purpose by reducing the crossflow disturbance vortex growth distance or time, i.e., decelerating the flow over a particularly short chordwise distance. At the same time the corresponding crossflow Stokes layer is thinner, shifting the maximum crossflow velocity closer to the surface to raise accordingly χ_{min}.

Crossflow stabilization in the rear pressure rise areas of the upper and lower surface is optimized by avoiding amplified crossflow disturbance vortices in the upstream part of the pressure rise. This is possible by sufficiently strong local suction in this region, such that the local Re_n is kept close to the corresponding χ_{min}. The crossflow disturbance vortices can then grow to its transition value at the termination of the rear pressure rise at the trailing edge (fig. 8).

This is not possible on the rear lower surface where the crossflow generated in its rear pressure rise area continues into the downstream high pressure zone to contribute a further crossflow disturbance vortex growth, even though no additional boundary layer crossflow is contributed by a pressure rise in this area. The crossflow on the rear lower surface must then be stabilized by sufficiently strong local suction towards the termination of its rear pressure rise at x/c = 0.86 for airfoil X66 such that the local Re_n is not appreciably larger than the corresponding χ_{min}, thereby avoiding an excessive growth of $n_{crossflow}$ between x/c = 0.86 and 1.0. Higher overall suction rates are then needed, raising accordingly the equivalent suction- and profile drag. Alternately, a local flow acceleration may be added in a "corner" area on the lower surface downstream of 0.86c for partial crossflow cancellation and reduction of $n_{crossflow}$ between x/c = 0.86 to 1.0. Additional weak suction may be needed in the high pressure zone of the rear lower surface to avoid amplified TS- disturbance growth and a possible adverse interaction with amplified crossflow- disturbances.

The termination of the rear pressure rise on the lower surface at x/c = 0.86 thus requires increased suction for full chord laminarization. The resulting increase in equivalent suction- and profile drag is, therefore, a consequence of the airfoil aft loading, which in turn is due to the design towards high $M_{\infty_{Design}}$ (without such aft loading either $C_{L_{Design}}$ or $M_{\infty_{Design}}$ would be lower). Similarly, the front loading on the lower surface, desirable to maximize $M_{\infty_{Design}}$ and at the same time avoid excessive wing pitching moments, leads to a strongly accelerated flow on the lower surface to further aggravate the boundary layer crossflow problem, whether the acceleration is accomplished in a 2-step acceleration (X66 airfoil) or a long gradual one. Relatively strong local suction is thus needed to

control crossflow around the second acceleration zone of airfoil X66. Likewise, a long gradual acceleration on the front lower surface would require relatively strong suction in this area over a considerable distance for crossflow control. Thus, the design towards high $M_{\infty_{Design}}$'s inevitably raises the equivalent suction- and profile drag of the lower surface.

The equivalent wing profile drag C_{D_∞} (including the equivalent suction drag $C_{D_{suction}}$, adding 10% for suction duct- and mixing losses) at $Re_c = 3 \times 10^7$ are for

$$\phi = 23^0 \; M_{flight}=0.83$$
$$C_{D_{\infty_u}} = 0.488 \times 10^{-3}, \; C_{D_{\infty_l}} = 0.478 \times 10^{-3},$$
$$C_{D_{\infty_{total}}} = 0.966 \times 10^{-3}$$

$$\phi = 37^0 \; M_{flight}= 0.97$$
$$C_{D_{\infty_u}} = 0.505 \times 10^{-3}, \; C_{D_{\infty_l}} = 0.515 \times 10^{-3},$$
$$C_{D_{\infty_{total}}} = 1.02 \times 10^{-3}$$

As compared to SC wings with partially and especially fully turbulent flow these profile drags are extremely low. As compared to equivalent unswept LFC wings $C_{D_{\infty_{total}}}$ is about 20% higher, due primarily to the relatively large percentage drag contribution of the lower surface, being equal to that of the upper surface (with the lower flow velocities on the lower surface, its C_{D_∞}- contribution should be about 25% lower than for the upper surface of an unswept all laminar LFC wing). The relatively large C_{D_∞}- contribution of the lower surface is thus a consequence of the design compromises towards high $M_{\infty_{Design}}$ without excessive negative wing pitching moments.

For X66 type SC LFC airfoils without suction in the rear pressure rise areas (but with a slotted small chord trailing edge cruise flap), extensive laminar flow back to 70% and $C_{D_\infty} = 0.0025$ to 0.0030 appear possible at $Re_c = 3.0 \times 10^7$. C_{D_∞} could decrease 20% by extending suction laminarization downstream of the main wing structural box for a short distance into the rear pressure rise zone at relatively modest additional suction rates.

C. Three Dimensional Airplane Design Integration

Optimum upper surface pressure distributions with high design Mach numbers on tapered swept SC wings.

With wing sweep needed to raise the design Mach number of high subsonic speed LFC transports, the question arises concerning the pros and cons of tapered swept-forward or swept- back wings from the standpoint of design Mach number, laminarization, and structural and aeroelastic characteristics. A decisive aerodynamic advantage of tapered swept-forward LFC wings is the reduction in the leading edge sweep. Crossflow- and attachment line boundary layer instability as well as leading edge contamination by flyspecks and atmospheric ice crystals are thus alleviated.

Taper of swept wings modifies the optimum chordwise C_p- distribution for a high design Mach number: On tapered swept-back or swept-forward SC wings the isobar sweep decreases or increases, respectively, from the wing leading- to the trailing edge, superimposing an additional streamwise flow deceleration or acceleration, respectively, when the flow Mach number component in the direction normal to the isobars is kept constant, as seen in the figs. 11,12 for $M_{flight} = 0.83$ and 0.98. With this additional flow acceleration on tapered swept-forward LFC wings the boundary layer in the flat rooftop area of the upper surface is more stable with respect to amplified TS-disturbances, as compared to a 2-dimensional yawing wing of the same sweep; vice versa, TS-disturbances on tapered swept-back wings are more strongly amplified as a result of the taper-induced flow deceleration. Assuming upper surface isobars along constant percentage lines, a tapered swept-back SC LFC wing with X66-type SC airfoils, optimized for a high cruise Mach number, will have a sloping down upper surface rooftop pressure distribution, preceded by a more pronounced supersonic pressure minimum (fig. 13), as compared to an equivalent yawing wing. Additional spanwise suction strips may then be needed in this flow deceleration area of the upper surface rooftop for further boundary layer stabilization against amplified TS-disturbances. The additional suction rates required for this purpose are small and can be applied in relatively narrow suction strips. Of course, a tapered swept-back SC LFC wing does not necessarily have to be designed with such a decelerated flow on the upper surface for the cruise design point, at a corresponding penalty, though, in $M_{\infty_{Design}}$.

In contrast, assuming upper surface isobars along constant percentage lines, a tapered swept-forward SC LFC wing with X66 type SC airfoils will have an optimum design pressure distribution for high $M_{\infty_{Design}}$ with slightly accelerated flow (fig. 13). This will reduce the growth of TS-disturbances in the rooftop area of the upper surface.

The question arises as to how to further raise $M_{\infty_{Design}}$ and $C_{L_{Design}}$ of tapered swept-back and swept-forward SC LFC wings. This is possible 1) by increasing the upper surface isobar sweep over the constant percent chord line sweep, 2) by a favorable 3-dimensional aerodynamic design integration of the airplane configuration and its components at high subsonic speeds.

1) Since the isobar sweep at the start of the rear pressure rise on the upper surface is equal to the sweep angle of a possible shock front during cruise, $M_{\infty_{Design}}$ would increase by raising this isobar sweep over the sweep angle of the local constant percent chord line. On a tapered swept-back wing this is, in principle, possible by shifting the start of the rear pressure rise further forward in the inboard and further aft in the outer wing, and vice versa on a tapered swept-forward wing, accomplished by suitably tailoring the airfoil sections along the span. When the rear pressure rise of the upper surface is thus shifted further aft in the inboard area of a tapered swept-forward wing, where wing bending- and torsional moments are largest, the local $M_{\infty_{Design}}$ increases further, and vice versa for a tapered swept- back wing. In the outer part of a swept-forward wing, where the structural loads are much less critical, somewhat thinner SC airfoils are easily feasible with but minor wing weight penalties to compensate for the loss in $M_{\infty_{Design}}$ due to the earlier pressure rise on the upper surface. It thus appears well worth to raise $M_{\infty_{Design}}$ of tapered swept-forward SC wings by increasing the isobar sweep at the start of the rear pressure rise on the upper surface over the corresponding sweep angle of the local constant percent chord line. In contrast, relatively little can thus be gained in $M_{\infty_{Design}}$ for tapered swept-back SC wings.

To further increase the design Mach number of tapered swept- forward wings it would be ideal if the same isobar sweep could be maintained over most of the upper surface not only at the start of the rear pressure rise but also further upstream into a zone where off-design shocks at lower M_∞'s start far upstream, when the upper shock-free low drag C_L- limit starts dropping. This is possible by tailoring the SC airfoil sections in the outer wing close to of the external fuel nacelle such that the upper surface pressure minimum in this area is located especially far upstream, followed by a particularly rapid flow deceleration, combined with slightly lower (t/c)'s and C_L's. The upper surface isobars are thus pulled further upstream in the front part of the outer wing to increase accordingly the local isobar sweep angle and maintain a larger isobar sweep over a substantial percentage of the upper surface. The upper surface static pressures decrease further over most of the upper surface (fig. 13) to raise either $C_{L_{Design}}$ (at given M_∞ and ϕ) or M_∞ (at given $C_{L_{Design}}$ and ϕ).

Since the resulting upper surface rooftop C_p-distribution will be more flat and its boundary layer accordingly more sensitive to TS- disturbances, this approach is of particular interest to swept-forward SC LFC wings in advanced composite structure with several narrow suction strips in the rooftop area.

Figure 14 shows the design KG-plot of such a modified SC LFC airfoil with a particularly sharp front pressure minimum. The corresponding upper surface hodograph streamline (fig. 14) slopes down especially slowly and continuously over a surprisingly wide range of flow inclination angles. As a result, the upper shock-free low drag C_L-limit extends to relatively high C_L's over a wide M_∞-range (fig. 15). With respect to the upper shock-free low drag C_L-limit this airfoil is superior over SC LFC airfoils with an extensive flat rooftop without a front pressure minimum (fig. 16).

With this approach the resulting isobar sweep over most of the upper surface of tapered swept-forward SC LFC wings is then considerably larger than the structural sweep. In contrast, this is not as easily possible with swept-back SC LFC wings. Thus, swept-forward wings may be designed with larger aerodynamic spans (for a given structural span) and correspondingly lower induced drag, provided, though, that wing divergence is delayed far beyond any flight dynamic pressures to minimize or preferably eliminate additional divergence induced wing gust loads. For composite wings this is possible at a relatively minor structural weight penalty by sweeping the spanwise bending fibers ahead of the elastic axis, strut-bracing the wing against bending and torsion, sweeping the wing outboard of the external fuel nacelle back and actively controlling wing bending- and torsional deformations in gusts by the cruise flap and the control surface of the external fuel nacelle.

2) $M_{\infty_{Design}}$ or $C_{L_{Design}}$ of the airplane increases further if it should prove possible to reduce the Mach number component normal to the upper surface isobars and thereby lowering C_p especially on the front upper surface of high subsonic speed LFC airplanes with swept-forward wings (especially when cruising close to M = 1). This appears possible with a favorable 3-dimensional aerodynamic integration of the airplane configuration and its components. Negative perturbation velocities can be induced on the upper wing surface (especially in its front part) by suitably located laminarized superfan- and fuel- or outrigger gear nacelles, mounted upstream of the wing, and integrating the wing design with these nacelles and the fuselage. Alternately one may look at the problem as follows: With a carefully laid out individual area ruling of each of these nacelles with the corresponding local wing, combined with additional local streamline contouring and a proper area-ruling of the entire airplane configuration, the combination of wing plus nacelles behaves then especially at very high subsonic speeds close to $M_\infty = 1$ to a first approximation as if the wing thickness were essentially distributed over the entire length from the nacelle leading edges to the wing trailing edge.

The wing thickness induced perturbation velocities thus decrease substantially to further increase $M_{\infty Design}$ of such a 3-dimensionally integrated airplane configuration (fig. 17). In principle, the same approach is possible for swept-back airplane configurations, placing the superfan- and fuel- or landing gear nacelles downstream of the wing trailing edge similar to Whitcomb's bumps. Wing flutter, though, may then be critical. The above described 3-dimensional integration of wing and nacelles is worthwhile, though, only if such nacelles are needed anyhow, or if they alleviate wing structural loads and deformations, and especially if extensive laminar flow can be maintained on these nacelles and the wing by suitable boundary layer control.

With such an approach a careful study of the flow interference between the wing and nacelles and their supporting struts is needed to ensure satisfactory pressure distributions on the wing, nacelles and struts.

The first author is indebted to R.T. Jones, H. Lomax, J. Spreiter, R. Whitcomb and P. Rubbert for many valuable discussions on these 3-dimensional integration concepts.

D. Propulsion Considerations

The question arises concerning the choice of the cruise propulsion system from the standpoint of a high overall efficiency $\eta_{overall}$ and reduced acoustic disturbances, particularly in the range of strongly amplified TS- and other types of boundary layer disturbances on the laminarized airplane surfaces, which might adversely affect airplane laminarization****. This is particularly important for LFC airplanes with extensive natural laminar flow in the flat rooftop area of the upper surface without the stabilising influence of distributed suction. (Distributed suction along the entire chord strongly stabilises the boundary layer to allow correspondingly increased initial disturbances.) Of course, propulsion induced disturbances are inherently less critical for aerodynamically efficient airplanes with high (L/D)'s due to their lower propulsion power.

Up to M_{cruise}= 0.80 nonregenerative high pressure ratio turboprops, driving high speed counter-rotating propellers, are superior in $\eta_{overall}$ over turbofans. Propeller tone noise frequency is usually below the frequency range of strongly amplified TS-waves on the wing, and, therefore, propeller tone noise does not appear critical in this respect. Its frequencies, though, are in the range of amplified travelling crossflow- or highly oblique TS- disturbance vortices in the rear pressure rise area of all laminar swept LFC wings to possibly induce amplified travelling boundary layer crossflow disturbance vortices.

Beyond M_{cruise}= 0.80 the compressibility problems of the propeller blades can be alleviated by installing the propeller in the decelerated internal flow field of a duct (or possibly in the decelerated rear flow field of a fuselage), especially if extensive laminar flow by means of suitable geometry and suction can be maintained on the external duct surfaces and even in the fan inlet up to the fan rotor. Such a ducted propeller or superfan (bypass ratio 15 to 20) was first proposed by Ackeret in 1938. The fan blades rotate then at relatively low tip speeds to allow accordingly a substantial axial decay of the rotating fan rotor pressure field and of many rotating fan rotor-stator acoustic interference modes in the fan duct. Most of the tone noise of the superfan is generated at frequencies considerably below those of amplified TS-oscillations but above those of amplified travelling boundary layer crossflow disturbance modes in the rear pressure rise area of all laminar swept LFC wings. In contrast, the present high bypass ratio turbofans of bypass ratio 5 to 6 contribute a substantial percentage of their tone- and shock noise in the frequency range of strongly amplified TS-oscillations on the wing.

It is not clear whether to favor directly driven aft-mounted counter- rotating ducted propellers (or superfans), as proposed by Rolls- Royce [Ref. 13], or geared front superfans. The Rolls-Royce approach could allow a 3-speed gas generator to thus enable increased engine pressure ratios with correspondingly higher thermodynamic efficiencies. Furthermore, avoiding the large diameter fan shaft in the gas generator with a rear-mounted superfan permits larger blade dimensions and correspondingly higher stage efficiencies especially in the high pressure compressor spool [Ref. 13].

An aft- mounted superfan might be preferable over a front- mounted superfan in generating negative thrust during landing without seriously affecting the flow into the gas generator, when the fan blades are set into reverse pitch. The problems involved with the generation of negative thrust by reversing the fan blade pitch were brought to the attention of the first author by K. Schuppisser of Boeing. These problems would not occur to the same degree with an open propeller.

**** With the atmospheric microscale turbulence being usually too weak to affect transition, the initial disturbances introduced into the boundary layer are created primarily by the airplane itself and especially its propulsion system as well as suction induced disturbances.

With the tone noise frequency of the superfan essentially below the frequency range of amplified TS-disturbances on the wing, such a superfan may be mounted in front of the wing without seriously affecting wing laminarization. To alleviate compressibility problems particularly on the external fan nacelle surfaces and at the same time minimize fan air exit shock noise, especially at near sonic cruising speeds (M_∞= 0.97 LFC transport), the fan nacelle inlet and exit may have to be sufficiently swept parallel to the wing (as seen in planview). On both sides of such swept nacelle inlets and exits the flow is similar as at the wing-fuselage juncture of a swept-back and swept-forward wing. To maintain shock-free flow in these areas, local area-ruling and streamline contouring is needed as in the wing-root area of a high speed airplane with a waisted fuselage, using body fairings which extend on both sides of the fan nacelle for a considerable distance fore and aft of the fan inlet and exit (see example of M_{cruise}= 0.97 airplane, fig. 17).

In addition, the superfan nacelle, located upstream of the wing in the area of the wing-strut juncture, combined with the fuel nacelles (figs. 1 and 17), induces a negative perturbation velocity in the area of the downstream wing. Either a thicker wing is thus possible especially in the area of the wing-strut juncture, where the wing bending moments are largest, or a larger wing span with lower induced drag could be used, thereby partially compensating for the nacelle parasite drag.

Figure 18 shows the variation of the engine thermodynamic and overall efficiency of the propeller and superfan versus flight Mach number for nonregenerative high pressure ratio gas-turbine engines, driving high speed counter-rotating propellers and superfans (high component efficiencies were assumed). Up to M_{cruise}= 0.83 the turboprop is superior over the superfan, while at higher speeds the superfan engine has higher $\eta_{overall}$. Other aspects, though, (blade containment, engine location, weight, etc.) affect the choice of the propulsion system.

For the M_{cruise}= 0.83 and 0.97 LFC airplanes of W_o = 180,000 Kg take-off gross weight wing mounted superfans of the Rolls-Royce type with about 18,000 Kg take-off thrust were selected, combined with a fuselage boundary layer propulsion engine in the rear fuselage (assuming a turbulent fuselage). The equivalent turbulent fuselage drag may thus decrease by 10%. Its gas generator is fed with undisturbed ram air.

Since the thrust produced by the suction compressors contributes particularly efficiently to the total cruise thrust of an LFC airplane they should be driven by thermodynamically highly efficient and not by thermodynamically inferior engines, i.e. either directly from the main propulsion engine via a mechanical or perhaps a bleed and burn cycle drive, possibly with regeneration. At lower flight speeds the suction compressors should preferably be geared down to reduce their power input. If separate smaller suction drive engines are considered either high pressure ratio nonregenerative or better yet particularly efficient low pressure ratio regenerative engines with a highly efficient regeneration should be chosen. Accepting 70% laminar flow on wing, empennage, struts and tail surfaces (turbulent fuselage), relatively limited suction is needed in the front part of these surfaces, i.e. no suction is required in their rear pressure rise areas. A direct mechanical suction compressor drive from the main engines is then easily feasible.

E. Airplane Design Examples

The figs. 1 and 17 show examples of strut-braced M_∞= 0.83 and 0.97 LFC transport airplanes***** of W_o = 180,000 Kg take-off gross weight and 50,000 Kg payload (250 passengers plus cargo). 70% laminar flow was assumed over wing-, empennage-, strut- and nacelles surfaces with fully turbulent flow on the fuselage (60 meters long, ≈ 6 meters in diameter). Riblets and boundary layer propulsion reduce the equivalent fuselage drag by 7% and 10%, respectively. A swept-forward wing was chosen between the fuselage and the external fuel nacelle, while the outer wing is swept-back, primarily to alleviate wing divergence. At the same time the structural wing span of such an M-type wing is smaller than that of a fully swept-forward wing (for the same aerodynamic span), thereby reducing the bending moments in the inboard wing and allowing accordingly a somewhat larger aerodynamic span. This advantage, though, is bought at the price of an additional wing torsional moment induced in the inboard wing by the lift of the outer wing. In principle, this additional wing torsional moment can be partially compensated by a negative lift on the control surface of the external fuel nacelle. To avoid additional induced drag from this negative control surface lift, the sum of the wing- and control surface circulation should be chosen such as to minimize the induced drag of the total lift carrying system; for the same reason the vertical wake displacement of the wing and control surface should be kept small. The outboard wing is particularly thin to

***** Near sonic transport airplanes have been proposed and successfully tested in the 8-foot Langley Transonic Wind Tunnel by Whitcomb and his co-workers [Ref. 14] as well as by industry.

minimize local wing sweep and improve high speed buffeting towards the wing tip, where wing deflections are the largest.

Excessive pressure minima in the front part of the swept- forward wing towards the wing-fuselage juncture are alleviated by a suitable area-ruling of the fuselage or streamline contouring of the upper fuselage section in the area of the wing-fuselage juncture and reducing the wing sweep towards the root. This is feasible by reducing the wing thickness towards the fuselage, which in turn is structurally easily possible in view of the rapidly decreasing wing bending moments in the strut-braced inboard wing area. At the same time C_{D_∞} of this thinner inboard wing decreases somewhat to partially compensate for the strut parasite drag.

The rapid reduction of the inboard wing thickness decreases at the same time the local Mach number of the upper wing surface in the area of the wing-strut intersection (the local flow is essentially 3-dimensional) to allow a correspondingly thicker wing in this structurally most critical area, where wing bending moments are the largest. Flow choking between the lower wing surface and the strut is avoided by suitable cutouts on the lower surface, using local area-ruling and streamline contouring [Ref. 1]. This was demonstrated in the Wright Field transonic wind tunnel on a strut-braced 35^0 swept wing airplane configuration of aspect ratio 9 with empennage and simulated nacelles (designed and built by the Northrop LFC research group). The measured lift to drag ratio (L/D) of the entire airplane configuration at M_∞= 0.89 and Re_c= 1.2 $\times 10^6$ was 21.2 [Ref. 15].

Wing mounted superfans, mounted in front and below the wing, combined with the external fuel nacelles, induce a negative perturbation velocity at the location of the wing to reduce essentially the local "free-stream" Mach number on the wing. The interaction of a high aspect ratio swept-forward and particularly thin wing towards the fuselage with the front-mounted superfan- and fuel nacelles enables a favorable cross-sectional area distribution of the airplane configuration with relatively minor area cutouts on the fuselage (see area distribution and fuselage contour of M = 0.97 LFC transports, fig. 19). A Reichardt type body of revolution was chosen for the equivalent body of revolution. Its calculated pressure distributions and supersonic bubbles are shown in fig. 20 for M=0.97 and 0.98.

A careful area distribution of the outer fuel nacelle with the thin outer wing enables a high local design Mach number in the juncture region of the wing and external fuel nacelle. The M_∞= 0.83 and 0.97 LFC airplanes require 23^0 and 37^0 aerodynamic wing sweep, respectively, at the start of the rear pressure rise. To maximize $M_{\infty_{Design}}$ the isobar sweep of the swept-forward wing is larger than the sweep angle of the constant percent chord lines. This can be accomplished by suitably tailoring the SC airfoils along the span (as discussed above).

With the larger wing sweep of the M = 0.97 (as compared to the M = 0.83 airplane) LFC airplane its span and aspect ratio decreases to raise $C_{D_{ind}}$ and reduce $(L/D)_{cruise}$ from 39.4 for the M_∞=0.83 airplane to 35. This reduction in L/D is partially compensated by a 3% higher powerplant overall efficiency. Tip feathers reduce the induced drag by about 8% (induced drag factor κ = 0.94 was assumed). Figure 21 shows a plot of L/D versus C_L for the M = 0.83 LFC airplane with wing aspect ratio of 19 and 70% laminar flow on wing, empennage, struts and nacelles (fuselage turbulent); with $(\frac{L}{D})_{max}$= 39.4 at $C_L \approx$ 0.6. One might reduce C_L somewhat to raise the cruise Mach number at a slight penalty in L/D. For comparison, fig. 21 shows L/D of the same airplane both with fully turbulent flow (L/D = 27.5) as well as with fully laminar flow on the wing, empennage, struts and nacelles by means of suction and various degrees of suction laminarization on the fuselage. With increasing fuselage laminarization L/D could increase substantially to exceptionally high values ($\approx$ 80) in the ideal case of 100% laminarization. Figure 22 shows a comparison of L/D and Re_c of the strut-braced M_∞= 0.83 airplane and a cantilever comparison LFC airplane (aspect ratio 12) versus C_L, showing superior (L/D)'s and substantially lower Re_c's for the strut- braced design. Assumptions for the M_∞= 0.83 airplane range estimate:

W_o = take-off gross weight = 180,000 Kg,
Payload = 50,000 Kg = 0.278 $\times W_o$,
Gross weight empty = 0.38 $\times W_o$,
Fuel reserves for take-off, climb, loitering, etc. = 0.06 $\times W_o$
$(L/D)_{average}$ = 37
Specific fuel consumption b = 0.48 Kg/Kg thrust

The resulting unrefuelled range is 21,564 kilometers = 11,606 nautical miles.

Figure 23 shows a plot of L/D versus C_L for the M = 0.97 near sonic LFC transport airplane with wing aspect ratio of 14.3 and 70% laminar flow on wing, empennage, struts and nacelles (fuselage turbulent); with $(\frac{L}{D})_{max}$= 35 at $C_L \approx$ 0.5. Figure 23 includes (L/D) versus C_L with fully laminar flow by means of suction on wing, empennage, struts and nacelles and various de-

grees of fuselage suction laminarization. Assumptions for the $M_\infty = 0.97$ airplane range estimate:

W_o = 180,000 take-off gross weight
Payload = 50,000 Kg,
Gross weight empty = $0.38 \times W_o$,
Fuel reserves = $0.06 \times W_o$
$(L/D)_{average} = 33$
$\eta_{overall}$ is 3 % higher than for the $M_\infty = 0.83$ airplane.

The resulting unrefuelled range of the near sonic M = 0.97 LFC transport is 19,810 kilometers (10,708 nautical miles),which is about 8% lower than for the $M_\infty = 0.83$ LFC transport.

Conclusions

70% laminar flow by means of modest boundary layer suction on wing, empennage, nacelles and struts of long range LFC transports, combined with lower span loadings and correspondingly larger wing spans, could enable an unrefuelled range halfway around the world up to near sonic cruise speeds with large payloads even with a turbulent fuselage. Increasing M_{cruise} from 0.83 to 0.97 reduces the range by 8.5%.

The structural weight of such large span wings critically affects airplane performance. It is minimized by bracing the wing externally with laminarized struts, alleviating wing bending loads by placing laminarized fuel nacelles in the outer wing with an active horizontal control surface.

The performance optimization by means of larger wing span is compatible with the desire to reduce wing chord- and unit length Reynolds numbers Re_c and $\frac{U_\infty}{\nu}$ for the alleviation of the laminarization problems involved.

Supercritical LFC airfoils with undercut front and rear lower surfaces and upper surface C_p- distributions with an extensive low supersonic flat rooftop, preceded by a far upstream supersonic overexpansion and followed by a steep subsonic rear pressure rise (either with suction or a slotted small chord trailing edge cruise flap) raise $M_{\infty_{Design}}$ and ease at the same time sweep- induced boundary layer crossflow instability on the upper surface.

Assuming equal $M_\perp$ (normal to the isobars) as on a constant chord wing, taper on sweptback wings adds a streamwise flow deceleration to aggravate their laminarization and require additional suction strips in their upper surface rooftop zone for TS- disturbance control. This effect is opposite for tapered swept- forward wings. Their isobar sweep at the rear shock location is larger than their structural sweep, thereby allowing increased wing span and lower induced drag than for equivalent sweptback wings. Of course, sweptforward wing divergence must be eliminated by sweeping the spanwise composite fibers ahead of the elastic axis, sweeping the outboard wing back and by means of active control, using for this purpose the cruise flap and fuel nacelle control surface.

$M_{\infty_{Design}}$ of tapered sweptforward LFC wings can be raised further by suitably tailoring the airfoils along the span, such that the upper surface isobar sweep is larger than the constant percent chord line sweep, as well as by a favorable 3- dimensional aerodynamic design integration of the airplane configuration and its components at high subsonic speeds.

In the high subsonic speed range wing mounted superfans, possibly combined with a fuselage boundary layer propulsion engine, reduce fuel consumption and engine tone noise in the range of amplified boundary layer disturbances. The fan nacelles can be used to reduce the local flow velocities in the area of the sweptforward wing and thus appear particularly attractive especially if their surfaces can be suction laminarized, provided the problems with negative thrust at landing can be solved satisfactorily.

References

1. Pfenninger, W., "Design considerations of large global range high subsonic speed LFC transport airplanes," AGARD-654, Agard/VKI Special Course on Concepts for Drag Reduction, Rhode-St. Genèse, Belgium, 1977.
2. Pfenninger, W., "Design considerations of long range and endurance LFC airplanes with practically all laminar flow," George Washington University Report, August 1982.
3. Whitcomb, R., and Clark, L., "An Airfoil Shape for Efficient Flight at Supercritical Mach Numbers," NASA TM X-1109, July 1965.
4. Gross, L. W., and Pfenninger, W., "Experimental and theoretical investigation of a Reichardt body of revolution with low drag suction in the NASA Ames 12-foot pressure tunnel," Northrop Report NOR63-46, BLC148, 1963.
5. Pfenninger, W., "USAF and NAVY sponsored Northrop LFC research between 1949 and 1967," AGARD-654, Agard/VKI Special Course on Concepts for Drag Reduction, Rhode-St. Genèse, Belgium, 1977.

6. Pfenninger, W., and Bacon, J. W., "About the development of swept laminar suction wings with full chord laminar flow," Boundary Layer and Flow Control, G. V. Lachmann, editor, Vol. 2, pp. 1007-1032, 1961.

7. Pfenninger, W., "Some results from the X-21 program. Part I: Flow phenomena at the leading edge of swept wings," Recent Developments in Boundary Layer Research, Agardograph 97, Vol. IV, Naples, May 1965.

8. Fowell, L. R., and Antonatos, P. P., "X-21 laminar flow control flight test results," Recent Developments in Boundary Layer Research, Part IV, Agardograph 97, Naples, May 1965.

9. Pfenninger, W., and Groth, E., "Low drag boundary layer suction experiments in flight on a wing glove of an F94A airplane with suction through a large number of fine slots," Boundary Layer and Flow Control, G. V. Lachmann, editor, Vol. 2, 1961.

10. Pfenninger, W., Viken, J. K., Vemuru, C. S., and Volpe, G., "All laminar SC LFC airfoils with laminar flow in the main wing structure," AIAA Design and Technology Meeting, Dayton, Ohio, AIAA 86-2625, October 20-22, 1986. Turbulence Management and Reattachment, H. W. Liepmann and R. Narasimha (Eds.), Springer-Verlag, IUTAM symposium, Bangalore/India, 1987.

11. Pfenninger, W., Reed, H. L., and Dagenhart, J. R., "Design considerations of advanced supercritical low drag suction airfoils," Viscous Flow Drag Reduction, edited by G. R. Hough, Vol. 72 of Progress in Astronautics and Aeronautics, 1980. Presented at the Symposium for Viscous Drag Reduction, Dallas, Texas, November 1979.

12. Malik, M., "COSAL - A black box compressible stability analysis code for transition prediction in 3-dimensional boundary layers,,, NASA Contractor Report 165925, Contract NAS1-16919, May 1982.

13. Lecture presented by the Rolls-Royce Chief Engineer at the Delft Technical University, September 1985.

14. Langhans, R. A., and Flechner, S. G., "Wind-tunnel investigation at Mach numbers from 0.25 to 1.01 of a transport configuration designed to cruise at near-sonic speeds," NASA TM-X-2622, August 1972.

15. Bacon, J. W., Fiul, A., and Pfenninger, W., "WADC 10-foot transonic wind tunnel tests on strut-braced boundary layer airplane," Northrop Report NAI-57-826, BLC-99, 1957.

Acknowledgements

The authors would like to thank Jerry Hefner, Branch Head of Civil Aircraft branch, Richard Wagner and Dal Maddalon of the Laminar Flow Control project office for their support. This work was sponsored by NASA Langley Research Center under contract NAS1-18235.

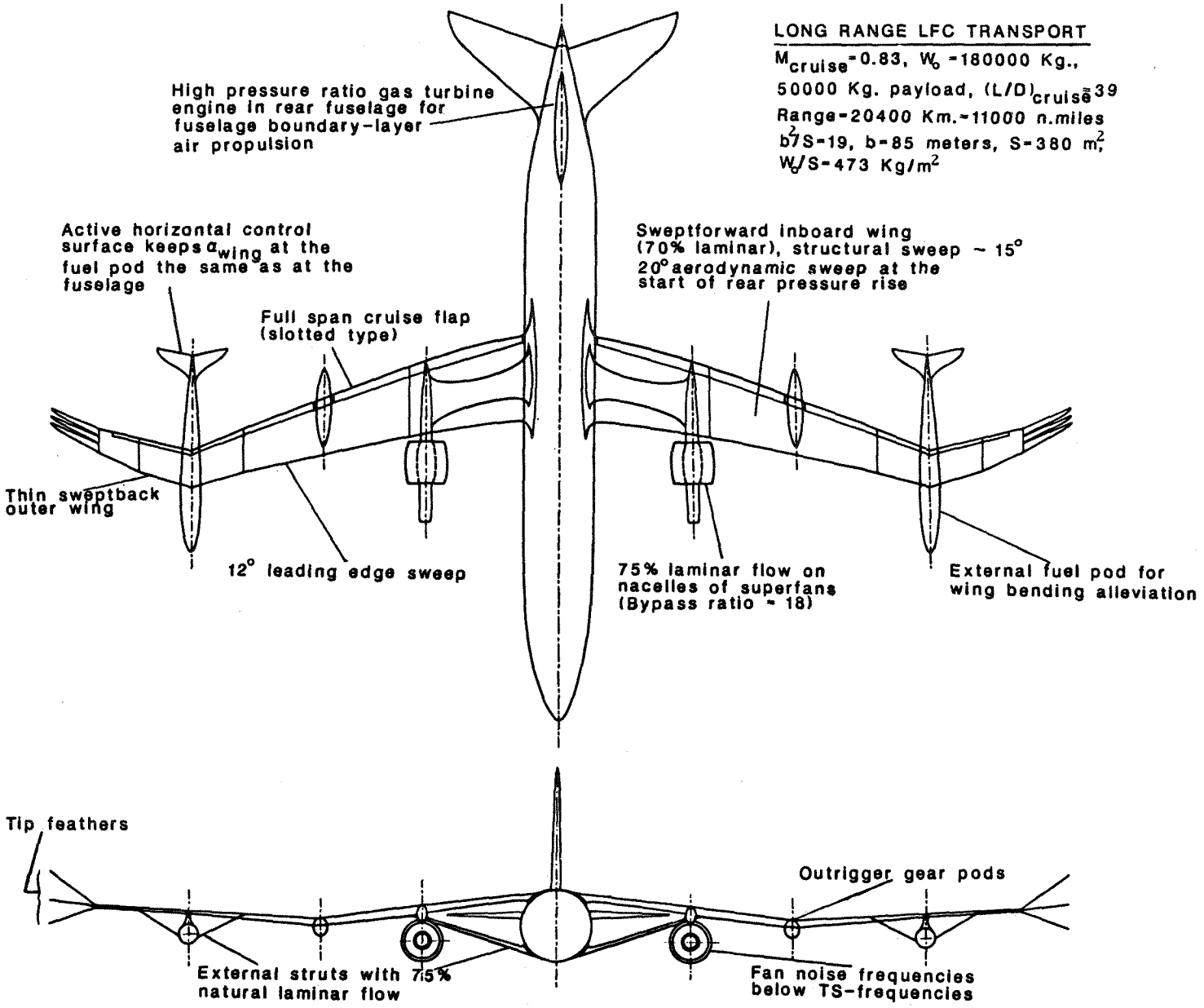

Fig. 1 $M_\infty = 0.83$ long range LFC transport airplane

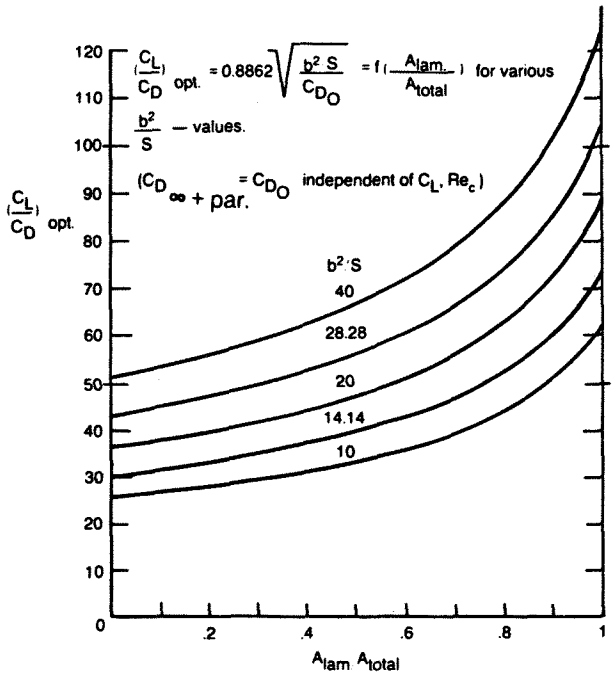

Fig. 2 $(C_L/C_D)_{opt}$ versus $A_{Laminar}/A_{Total}$ for various wing aspect ratios b^2/S, with $C_{D_o} = C_{D_\infty} + C_{D_{parasite}} = 0.012 - 0.01\,A_{Laminar}/A_{Total}$.

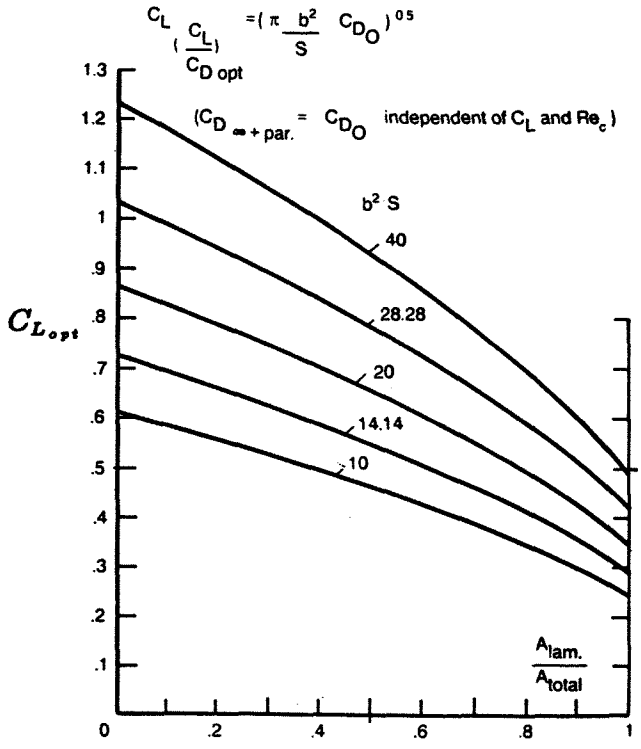

Fig. 3 $C_{L_{opt}}$ versus $A_{Laminar}/A_{Total}$ for various b^2/S values.

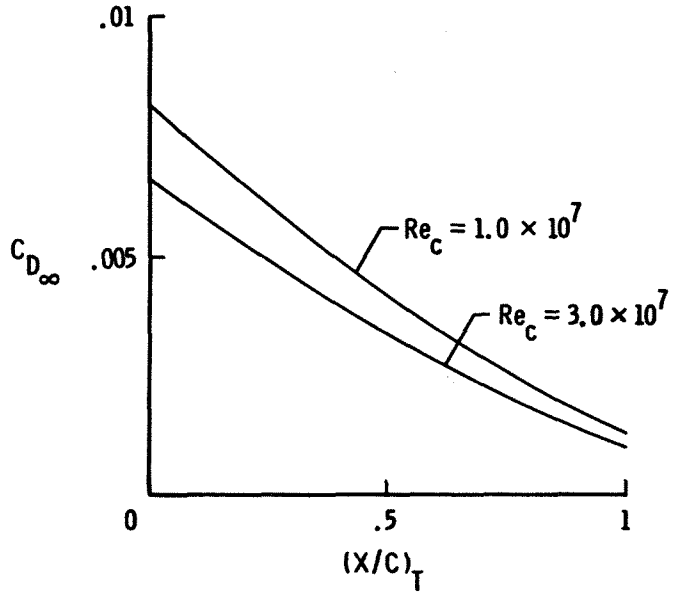

Fig. 4 Variation of C_{D_∞} with $(X/C)_{Transition}$ of 23° swept SC LFC airfoil for $Re_c = 10.0 \times 10^6$ and 30.0×10^6.

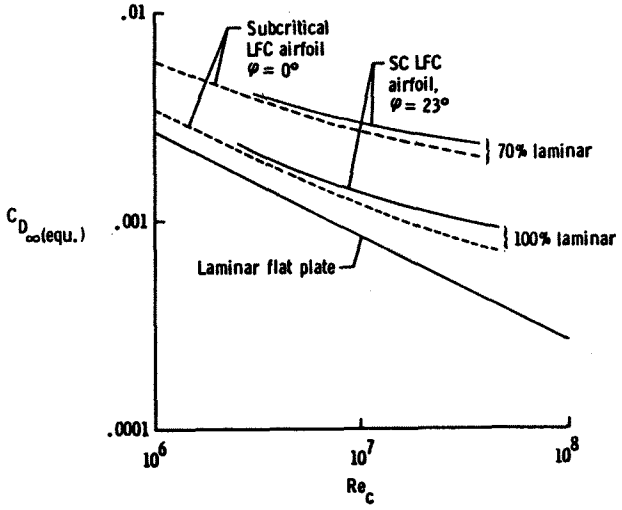

Fig. 5 Variation of C_{D_∞} with Re_c for $(X/C)_{Transition}$ = 0.7 and 1.0.

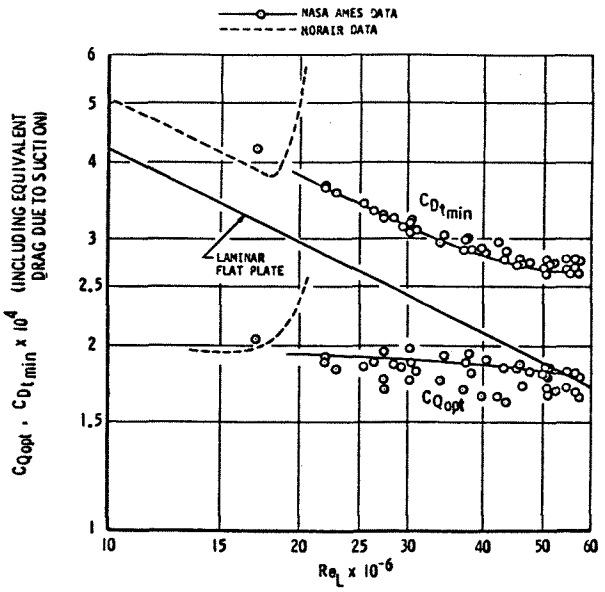

Fig. 6 $C_{Q_{opt}}$ and $C_{D_{t_{min}}}$ versus length Reynolds number for Reichardt LFC body of revolution.

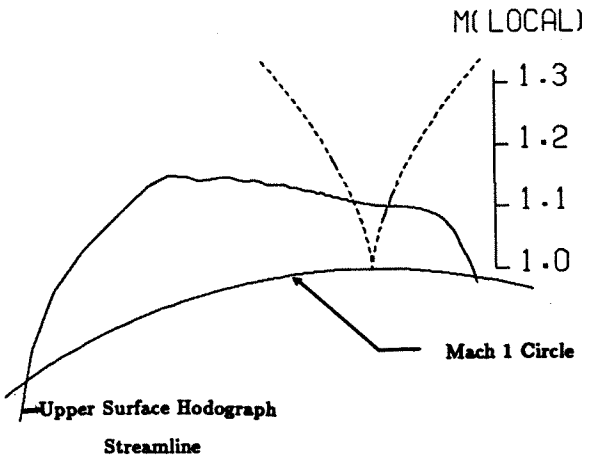

Fig. 7 (Concluded)

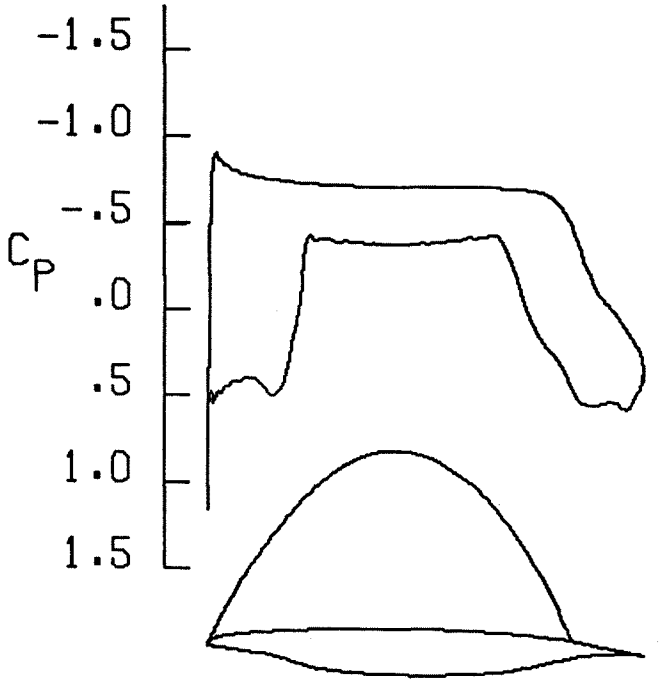

Fig. 7 Pressure distribution and hodograph plot for X66 SC LFC airfoil

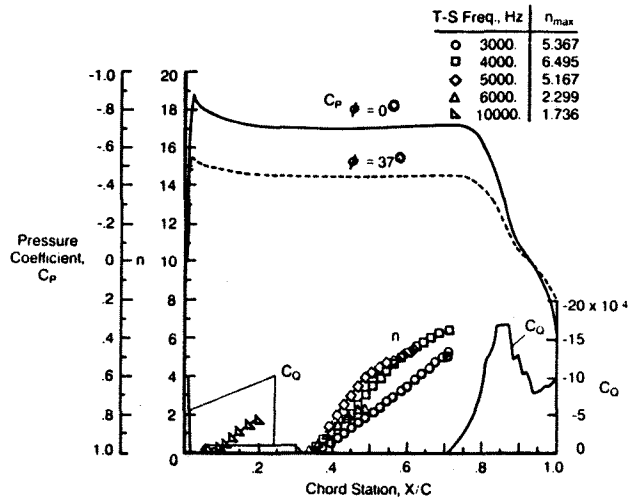

Fig. 8 X66 SC LFC airfoil at design: Boundary layer crossflow disturbance vortex growth and suction massflow distribution on upper surface for $\varphi = 37^0$ sweep, $M_\infty = 0.98$.

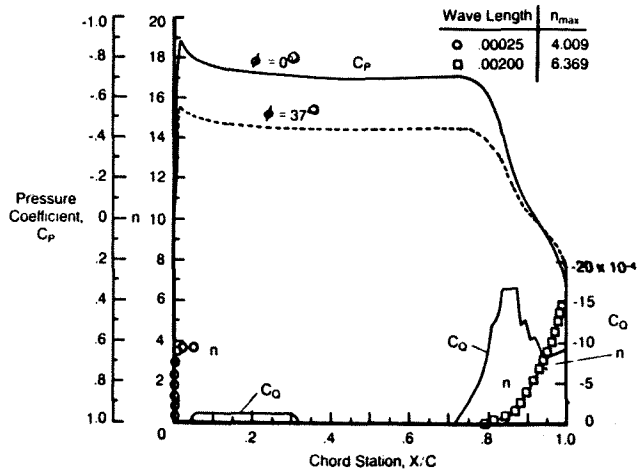

Fig. 9 X66 SC LFC airfoil at design: TS- boundary layer disturbance vortex growth on upper surface for $\varphi = 37^0$ sweep, $M_\infty = 0.98$.

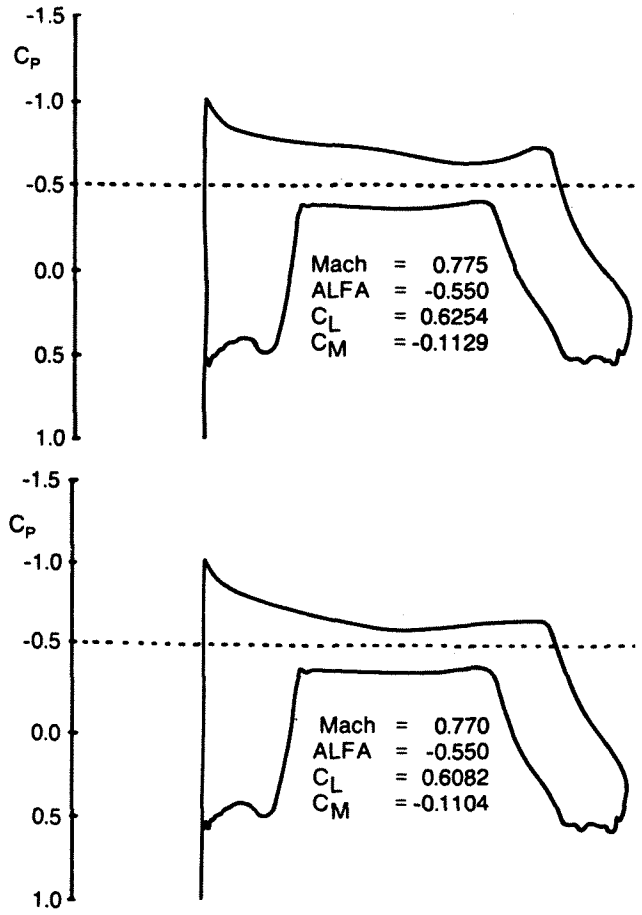

Fig. 10 Off-design C_p-distributions for modified X66 SC LFC airfoil

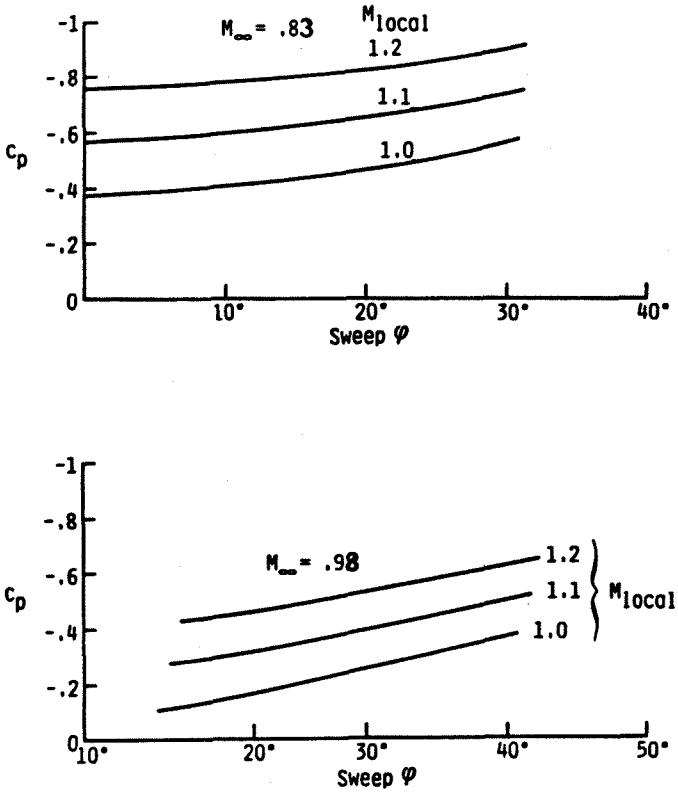

Fig. 11,12 Variation of C_p(based on q_∞) with isobar sweep φ for $M_\perp$ = constant, M_{flight} = 0.82 and 0.98.

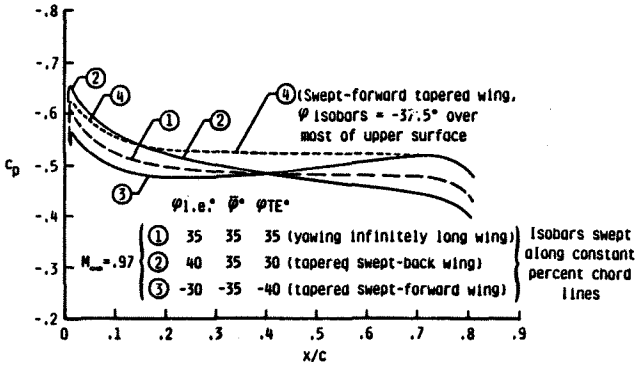

Fig. 13 C_p versus (X/C) for tapered sweptback and sweptforward wing with high $M_{\infty Design}$.

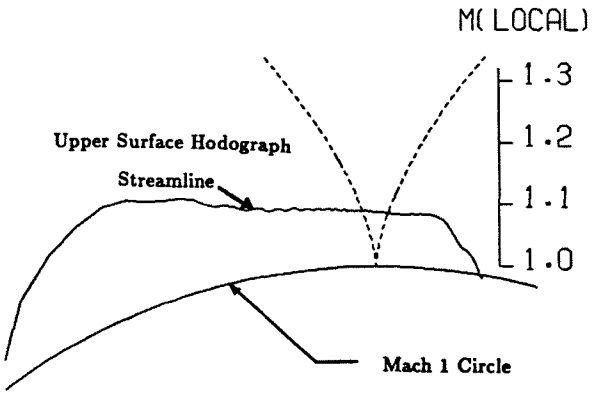

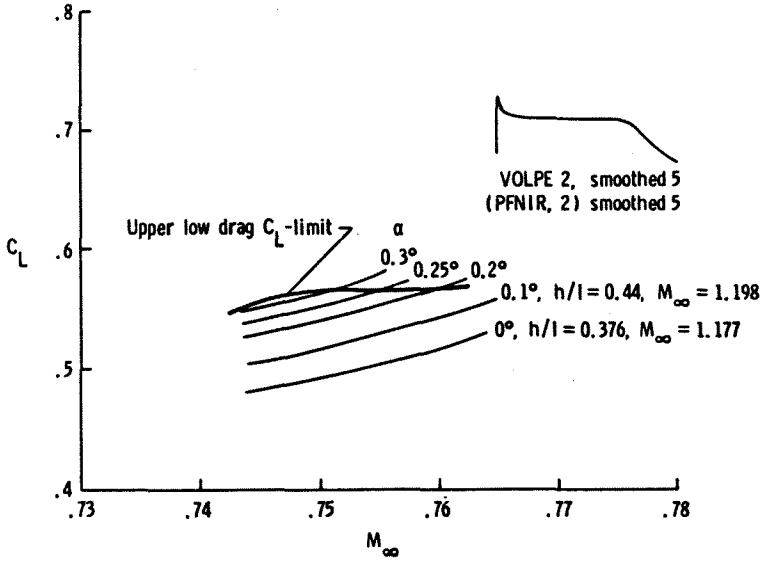

Fig. 15 Upper shockfree low drag C_L-limit for PFNIR2 SC LFC airfoil.

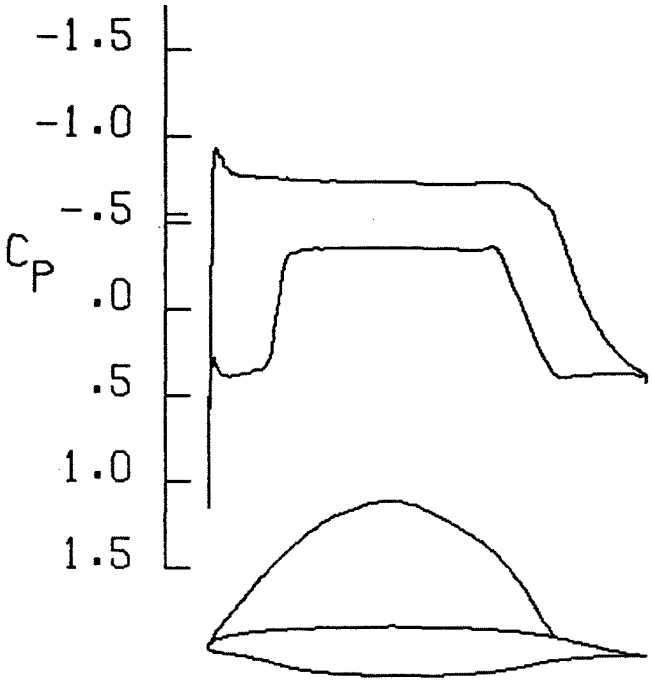

Fig. 14 Pressure distribution and hodograph plot for PFNIR2 airfoil.

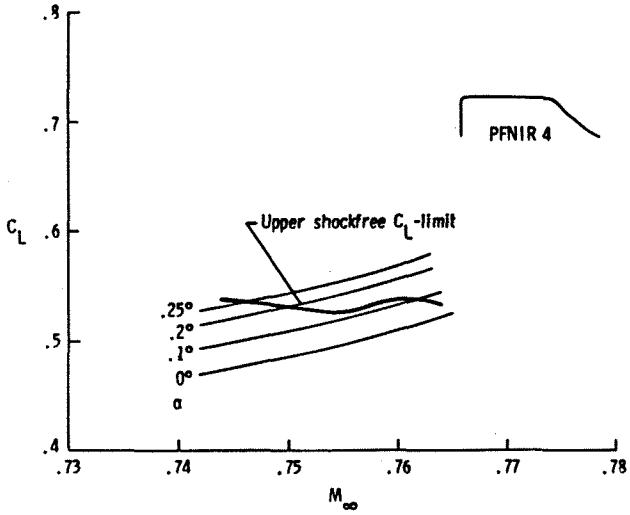

Fig. 16 Upper shockfree low drag C_L-limit of SC LFC airfoil without a front pressure minimum.

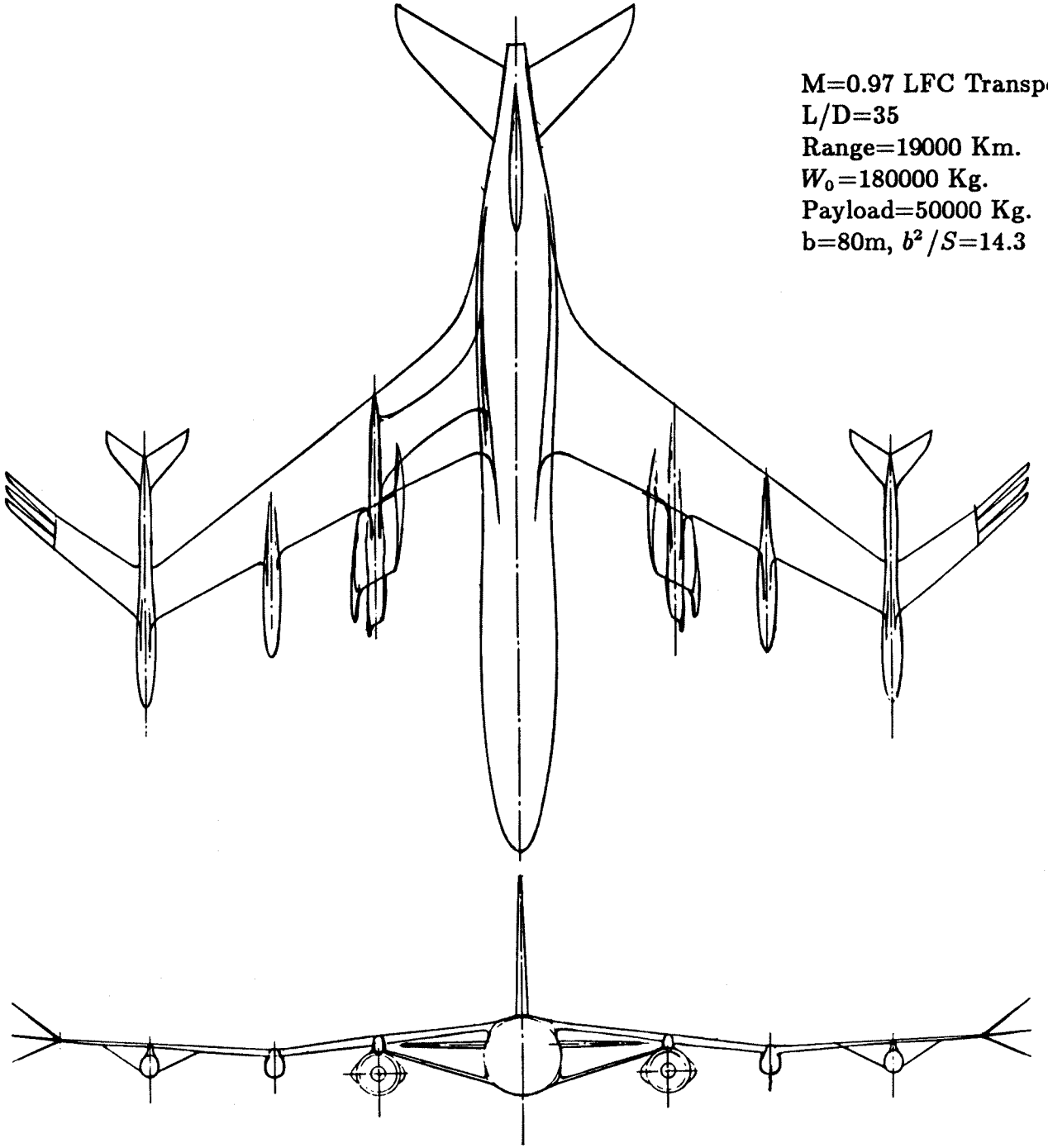

Fig. 17 $M_\infty = 0.97$ near sonic long range LFC transport airplane.

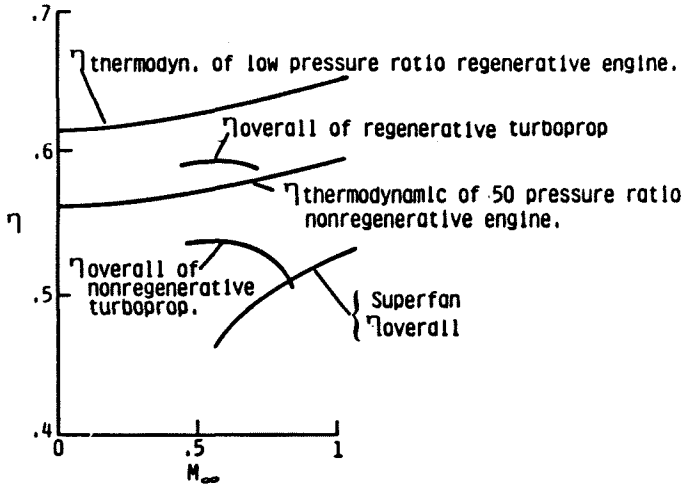

Fig. 18 Thermodynamic and overall efficiency versus M_∞ of superfans (BPR = 18) and high speed turboprops.

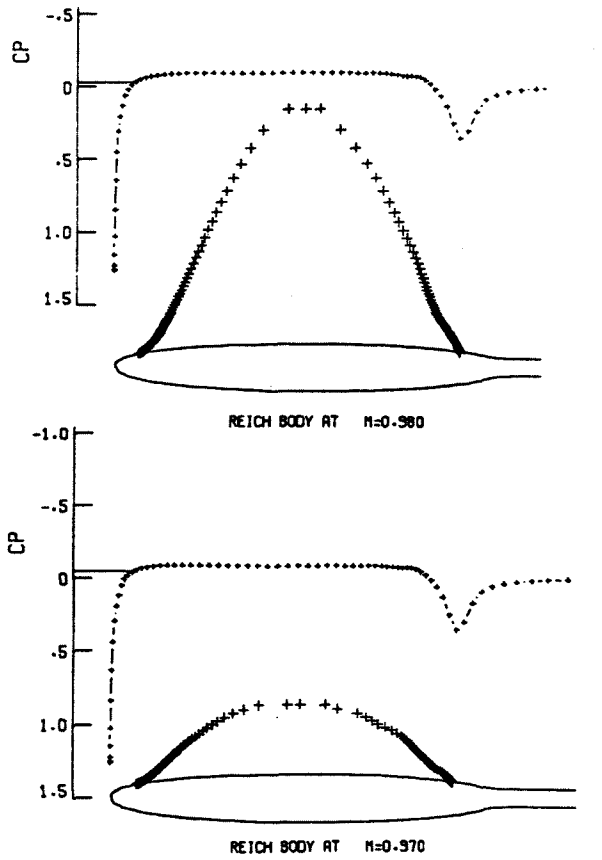

Fig. 20 Pressure distribution and supersonic bubble of equivalent Reichardt body of revolution at $M_\infty = 0.97$ and 0.98.

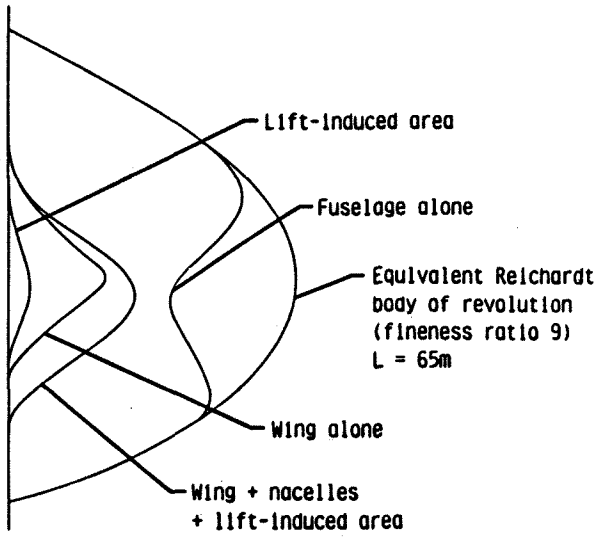

Fig. 19 Crossectional area distribution of $M_\infty = 0.97$ LFC transport (transonic area ruling).

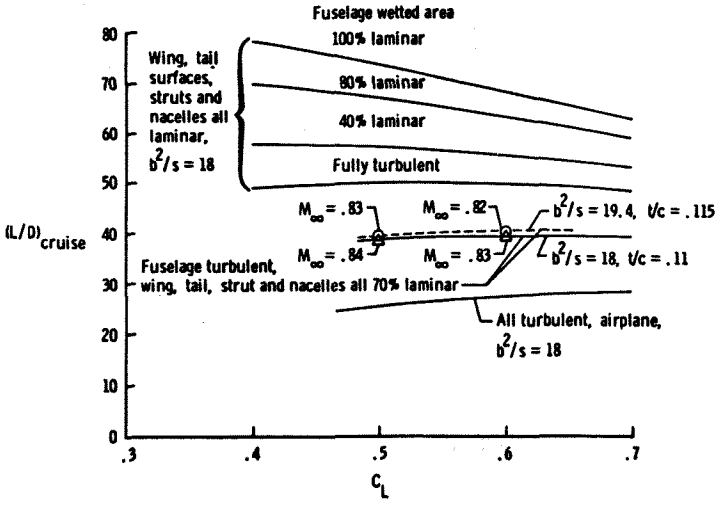

Fig. 21 $M_\infty = 0.83$ LFC airplane: $(L/D)_{cruise}$ versus C_L for different extents of laminar flow.

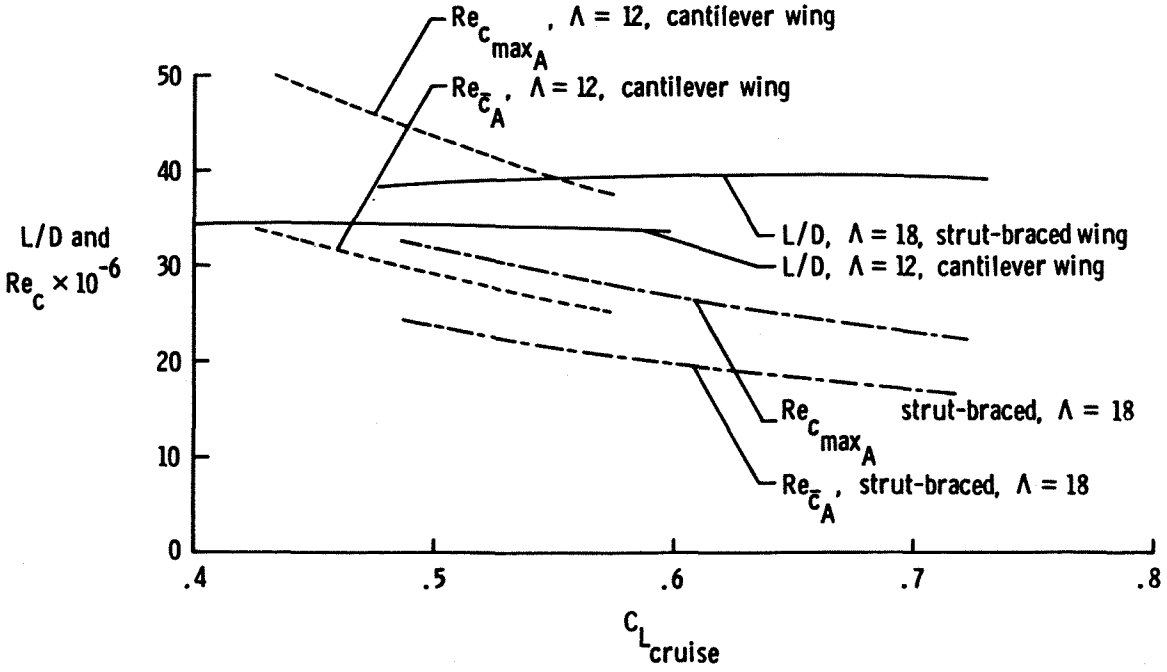

Fig. 22 $M_\infty = 0.83$ LFC airplane: $(L/D)_{cruise}$ and Re_c for strut-braced airplane ($b^2/S = 18$) and cantilever airplane ($b^2/S = 12$).

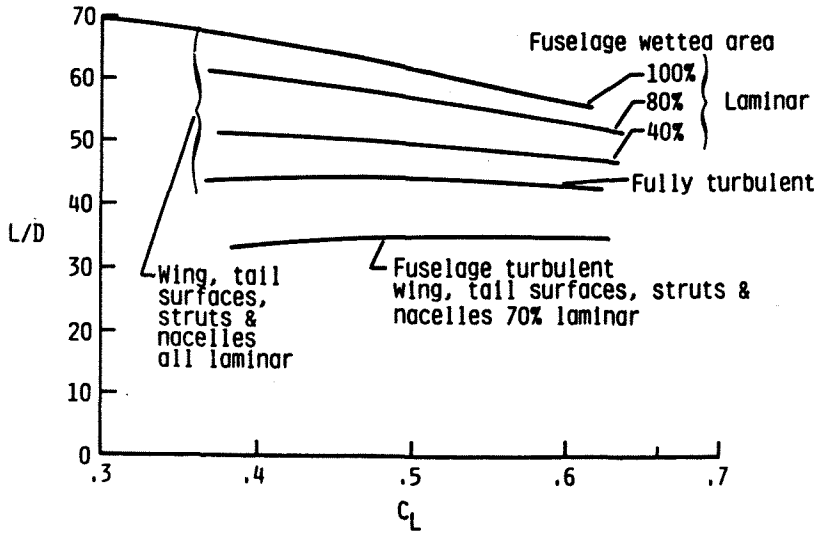

Fig. 23 $M_\infty = 0.97$ LFC near sonic LFC airplane: $(L/D)_{cruise}$ versus C_L for different extents of laminar flow.